Effect of Preparation Route and Thermal Treatment on the Nature of Copper and Chromium Doubly Promoted Ceria Catalysts

Philip G. Harrison,* Francis J. Allison, and Wayne Daniell†

School of Chemistry, University of Nottingham, University Park, Nottingham NG7 2RD, United Kingdom

Received January 18, 2001. Revised Manuscript Received July 18, 2001

Chromium and copper doubly promoted ceria catalysts have been prepared by three routes: (i) coprecipitation from aqueous solutions containing cerium(IV), copper(II), and chromium(III) ions, (ii) sequential impregnation of CeO_2 by using an aqueous CrO_3 solution followed by an aqueous solution of copper(II) nitrate, and (iii) impregnation of $Cu(II)/CeO_2$ prepared by coprecipitation by using an aqueous CrO_3 solution. The nature of the chemical transformations occurring during the thermal processing of the catalyst materials obtained by route (i) have been investigated by a combination of FT-IR, powder X-ray diffraction, transmission electron microscopy, X-ray absorption spectroscopy, and electron paramagnetic resonance spectroscopy. Some comparative data for materials obtained by the other two routes is also described. The nature of the transition-metal promoters varies substantially with the calcination processing temperature, the preparative route, and the Cu/Cr content. At low processing temperatures, copper is present as $Cu(OH)_2$ (polymeric) in the Cu/Cr/CeO_2-cop material, but a variety of chromium species in oxidation states +III, +V, and +VI are observed. After thermal processing at 573 K, the material comprises small crystallites of ceria-supporting amorphous copper(II) and chromium(III), chromium(V), and chromium-(VI) oxide species. Significant physical and chemical changes occur to the material by 873 K, which comprises crystallites of CeO_2 and the spinel $CuCr_2O_4$ which is converted at 1273 K to $Cu_2Cr_2O_4$, although a crystalline Cr_2O_3 phase separates with high chromium loadings. Chromium is present as adsorbed $\{Cr_2O_7^{2-}\}$ ions in the Cu/Cr/CeO_2-imp/imp and Cu/Cr/CeO_2-cop/imp materials at low-thermal treatments, but the dimeric surface anion is largely decomposed at 573 K although chromium(VI) is still present in substantial quantities. No ternary oxide phases are formed in either of these materials on thermal processing at high temperatures, and only phase-separated Cr_2O_3 and CuO are formed at temperatures from 873 to 1273 K.

Introduction

Catalyst materials that comprise both copper and chromium have been studied extensively for the oxidation of CO,[1−16] hydrocarbons,[1,17−19] sulfurated and chlorinated hydrocarbons,[20,21] and alcohols and aldehydes[22,23] as well as for NO reduction.[13,14,24] However, despite this quite large effort devoted to the study of Cu/Cr catalysts, the nature and constitution as well as the role of the constituents does not appear to be well understood. Many are referred to as "copper chromites",

* To whom correspondence should be addressed. E-mail: p.g.harrison@nottingham.ac.uk.

† Present address: Department Chemie, Physikalische Chemie, Ludwig Maximilians Universitaet Muenchen, Butenandtstrasse 5−13, 81377 Muenchen, Germany.

(1) Hertl, W.; Farrauto, R. J. *J. Catal.* **1973**, *29*, 352.
(2) Farrauto, R. J.; Hoekstra, K. K.; Shoup, R. D. U.S. Patent 3,-870,658, 1975.
(3) Kummer, J. T. *Adv. Chem. Ser.* **1975**, *143*, 178.
(4) Yu Yao, Y. F. *J. Catal.* **1975**, *39*, 104.
(5) Yu Yao, Y. F.; Kummer, J. T. *J. Catal.* **1977**, *45*, 388.
(6) Severino, F.; Laine, J. *Ind. Eng. Chem. Prod. Res. Dev.* **1983**, *22*, 396.
(7) Severino, F.; Brito, J.; Carias, O.; Laines, J. *J. Catal.* **1986**, *102*, 172.
(8) Laine, J.; Albornoz, A.; Brito, J.; Carias, O.; Castro, G.; Severino, F.; Vaiera, D. *Catalysis and Automotive Pollution Control*; Crucq, A., Frennet, A., Eds.; Elsevier: Amsterdam, The Netherlands, 1987; p 387.
(9) Laine, J.; Severino, F. *Appl. Catal.* **1990**, *65*, 253.
(10) Bijsterbosch, J. W.; Kapteijn, F.; Moulijn, J. A. *J. Mol. Catal.* **1992**, *74*, 193.
(11) Dekker, N. J. J.; Hoorn, J. A. A.; Stegenga, S.; Kapteijn, F.; Moulijn, J. A. *AIChE J.* **1992**, *38*, 385.
(12) Lopez Agudo, A.; Palacios, J. M.; Fierro, J. L. G.; Laine, J.; Severino, F. *Appl. Catal.* **1992**, *91*, 43.
(13) Kapteijn, F.; Stegenga, S.; Dekker, N. J. J.; Bijsterbosch, J. W.; Moulijn, J. A. *Catal. Today* **1993**, *16*, 273.
(14) Stegenga, S.; van Soest, R.; Kapteijn, F.; Moulijn, J. A. *Appl. Catal., B* **1993**, *2*, 257.
(15) Dekker, F. H. M.; Dekker: M. C.; Bliek, A.; Kapteijn, F.; Moulijn, J. *Catal. Today* **1994**, *20*, 409.
(16) Park, P. W.; Ledford, J. S. *Ind. Eng. Chem. Res.* **1998**, *37*, 887.
(17) Yu Yao, Y. F.; Kummer, J. T. *J. Catal.* **1977**, *45*, 388.
(18) Rastogi, R. P.; Singh, G.; Dubey, B. L.; Shukla, C. S. *J. Catal.* **1980**, *65*, 25.
(19) Chien, C. C.; Cheung, W. F.; Hueng, T. J. *Appl. Catal., A* **1995**, *131*, 73.
(20) Heyes, C. J.; Irwin, J. G.; Johnson, H. A.; Moss, R. L. *J. Chem. Technol. Biotechnol.* **1982**, *32*, 1034.
(21) Subbana, P.; Greene, H.; Desal, F. *Environ. Sci. Technol.* **1988**, *22*, 557.
(22) McCabe, R. W.; Mitchell, F. J. *Ind. Eng. Chem. Prod. Res. Dev.* **1983**, *22*, 212.
(23) Rajesh, H.; Ozkan, U. S. *Ind. Eng. Chem. Prod. Res. Dev.* **1993**, *32*, 1622.
(24) Tarasov, A. L.; Osmanov, M. O.; Shveta, V. A.; Kasanskii, V. B. *Kinet. Katal.* **1990**, *31*, 565.

10.1021/cm0110122 CCC: $22.00
Published on Web 01/16/2002

although it is not clear in many cases what is meant by the use of this terminology. Studies of Cu/Cr catalysts have reached a number of empirical conclusions. For instance, in such materials, copper oxide has been proposed to be the active component for CO oxidation while chromium oxide has been postulated to perform several functions including limiting catalyst reduction, preventing catalyst poisoning, inhibiting bulk copper aluminate formation, improving thermal stability, and increasing catalyst dispersion.[4,6−11,14,19,24,25] Synergistic effects have been proposed, which have been attributed to electronic interactions between the copper and chromium components.[6,10,19] What is also not well understood is the importance of the Cu/Cr ratio for optimum catalytic activity, and ratios of both 2 and 1 have been reported to be the optimum for CO oxidation.[7,26] In a series of Cu/Cr-promoted alumina catalysts, the formation of $CuCr_2O_4$ was demonstrated to give improved CO oxidation activity over CuO, while chromium-rich materials were less active due to the formation of Cr_2O_3.[16]

We have recently reported the activity of doubly promoted $Cu/Cr/CeO_2$ catalyst materials prepared by the coprecipitation route for the oxidation of carbon monoxide.[27] Thermal activation of this catalyst at 873 K produced sustainable 100% conversion at 403 K under stoichiometric conditions, but under lean burn conditions, 100% conversion could be maintained at 323 K. Treatment at 1273 K did not result in catalyst deactivation, which is a problem not uncommon with metal oxide based oxidation catalysts, but gave 100% conversion at 523 K.

The activity of catalysts can be critically dependent on several factors including the preparative route, composition and constitution, and the thermal history. A number of different routes are available in principle, but for a doubly promoted catalyst these fall into either (i) coprecipitation, (ii) impregnation of a preformed oxide material, or (iii) a combination of the two. In addition, a choice of different promoting metal precursors may be available. It might be expected that coprecipitation from solutions containing more than one metal cation would give rise to an oxide material in which the cations are uniformly dispersed within the freshly precipitated oxide particles. In contrast, impregnation will deposit the promoters on the surface of the oxide particles. Any subsequent thermal treatment will determine how the promoters will interact with each other and with the oxide support material. Many different changes, both chemical and physical, can occur during such thermal processing including sintering, change in pore texture, migration of hetero ions, phase separation etc. It is, therefore, of critical importance, for the understanding of the operation of this type of catalyst system, to gain a knowledge of their fundamental constitution and behavior on thermal treatment and highlight the differences in the constitution of the materials produced.

In this paper, we describe the nature of the doubly promoted $Cu/Cr/CeO_2$ catalyst obtained by coprecipitation after different thermal processing treatments. In addition, we explore two alternative routes to these catalyst materials.

Experimental Section

Preparation of $Cu/Cr/CeO_2$ Catalyst Materials. *(a) By Coprecipitation.* Catalyst preparation was achieved by a modification of the precipitation method described previously.[28] An aqueous solution of copper(II), chromium(III), and cerium(IV) nitrates in the target atomic ratios was stirred vigorously for 1 h to ensure an intimate mix of the three salts before addition of the aqueous ammonia/hydrogen peroxide solution. Hydrogen peroxide is present to ensure oxidation of Ce^{III} to Ce^{IV} during the precipitation process. This was achieved dropwise over a period of 1 h until pH 10 was reached. The mixture was stirred overnight at room temperature, after which the precipitate that was formed was washed by repeated centrifuging and redispersing in triply distilled water. The solid gel obtained was then allowed to air-dry at 333 K for 2−3 days. The dark brown materials prepared by this route are referred to as $Cu/Cr/CeO_2$−cop with the Cu:Cr:Ce atom ratio denoted in parentheses.

(b) By Dual Impregnation. Ceria was prepared by the ammonia precipitation method from an aqueous solution of cerium(III) nitrate hexahydrate. To this vigorously stirred solution was added a mixture of aqueous ammonia and hydrogen peroxide (10:1) dropwise over a period of 1 h until the solution reached pH 10. After the solution was stirred overnight at ambient temperature, the resulting yellow-brown precipitate was washed in triply distilled water and centrifuged three times. The solid was air-dried overnight at 383 K to give a pale yellow gel. The ceria powder so obtained was impregnated with Cr(VI), by stirring with a chromic acid solution (1.0 M) at 343 K for 18 h, filtered, and dried at 313 K overnight. The resulting yellow powder was then slurried in a solution of copper(II) nitrate in triply distilled water, stirred for 16 h at ambient temperature, and again left to dry at 313 K overnight. The light brown material prepared by this route is referred to as $Cu/Cr/CeO_2$−imp/imp with the Cu:Cr:Ce atom ratio denoted in parentheses.

(c) By Impregnation following Coprecipation. A $Cu(II)CeO_2$ (Cu:Ce, 20:80) material was first prepared by the coprecipitation method from a solution containing both copper(II) nitrate trihydrate and cerium(III) nitrate hexahydrate in triply distilled water. The mixture was stirred overnight at ambient temperature, after which the precipitate that was formed was washed by repeated centrifuging and redispersing in triply distilled water. The solid gel obtained was then allowed to air-dry at 333 K for 2−3 days. The dried oxide was subsequently impregnated with chromium(VI) by using a 2.0 M chromic acid solution. The bright orange material prepared by this route is referred to as $Cu/Cr/CeO_2$−cop/imp with the Cu:Cr:Ce atom ratio denoted in parentheses.

Elemental analytical data and observed and target Cu:Cr:Ce atom ratios for all materials are shown in Table 1.

Physical and Spectroscopic Measurements. Catalyst stoichiometries were determined by X-ray fluorescence (Philips PW1480 wavelength dispersive instrument). All spectroscopic data were obtained at ambient temperature after ex situ calcination (carried out at a heating rate of 10° per minute). Particular temperatures are indicated in the text. IR spectra were obtained by using a Nicolet 20SXC spectrometer fitted with a DTGS detector. From the KBr disk samples, 32 scans were recorded at a resolution of 1 cm^{-1}. Spectra are shown after subtraction of the air background.

Powder X-ray diffraction data was acquired by using a Philips X-pert system fitted with a PW 1710 diffractometer control unit with Cu Kα radiation ($\lambda = 1.5405$ Å). Representative diffractograms were acquired over 5−80° 2θ with 0.02° steps and 0.4 s acquisition times per step. DICVOL91[29] was

(25) Fattakhova, Z. T.; Ukharskii, A. A.; Shiryaev, P. A.; Berman, A. D. *Kinet. Katal.* **1986**, *27*, 884.

(26) Stegenga, S.; Dekker, N.; Kapteijn, F.; Moulijn, J. A. *Catalysis and Automobile Pollution Control II*; Crucq, A., Ed.; Elsevier: Amsterdam, 1991; p 353.

(27) Daniell, W.; Grotz, P.; Knozinger, H.; Lloyd, N. C.; Bailey, C.; Harrison, P. G. *Stud. Surf. Sci. Catal.* **2000**, *130*, 2183.

(28) Harrison, P. G.; Lloyd, N. C.; Daniell, W.; Bailey, C.; Azelee, W. *Chem. Mater.* **1999**, *11*, 896.

Table 1. Elemental Analytical Data

catalyst material	preparation route	target ratio Cu:Cr:Ce	metal content, wt % Cu	Cr	Ce	obsd atomic ratios Cr:Cu	Cu:Cr:Ce
$Cu/Cr/CeO_2$-cop	coprecipitation from aqueous solutions containing cerium(IV), copper(II), and chromium(III) ions	10:20:70	3.59	8.49	75.64	2.91	7.4:21.5:71.1
		20:20:60	6.18	9.50	67.56	1.87	12.7:24.0:63.3
		20:10:70	6.32	4.44	74.49	0.86	13.9:11.9:74.2
$Cu/Cr/CeO_2$-cop/imp	impregnation of $Cu(II)/CeO_2$-cop using an aqueous CrO_3 solution	20:10:70	5.44	7.01	72.62	1.62	11.6:18.3:70.1
$Cu/Cr/CeO_2$-imp/imp	dual impregnation of CeO_2 using an aqueous CrO_3 solution, followed by impregnation using an aqueous solution of copper(II) nitrate	10:10:80	3.12	3.62	83.73	1.43	6.8:9.7:83.5

used for indexing. Crystallite sizes were estimated by applying the Scherrer equation to the peak widths at half-maximum.

EPR measurements were recorded at 77 K by using a Bruker EMX EPR spectrometer equipped with a Bruker ER 041 XG Microwave bridge in X-band at ca. 9.2 GHz over a magnetic field range of 1000−5000 G. Experimental g values were determined with reference to diphenyl picryl hydrazyl (DPPH) ($g = 2.0036$).

X-ray absorption spectra were performed on station 8.1 at the Daresbury laboratory, Warrington, United Kingdom, which operates at an energy up to 2.0 GeV and a maximum beam current of 200 mA. EXAFS data were collected at the Cu K edge (8978.9 eV) in fluorescence mode utilizing a Ge-13 channel solid-state detector. The recording of EXAFS spectra at the Cr K edge (5989.2 eV) was not possible due to interference from the Ce L_{II} edge (6164.2 eV) and L_{III} edge (5723.4 eV). Hence, in this case, the study was confined to the monitoring of the changes occurring within the Cr species by observing preedge features in the XANES region. The sample was positioned at ca. 45° to the incident beam so as to maximize the solid angle seen by the detector. For each catalyst sample, 6 scans were recorded and refinement was achieved by using EXBACK, EXCALIB, and EXCURV92.[30] For a more detailed description of the curved wave theory used in the program to calculate theoretical backscattering amplitudes and phase shifts the reader is directed to the publications of Gurman[31] and Lee.[32]

The fit correlation parameter R between the calculated and observed data falls in the very acceptable range of 20−40. Values of $R < 50$ are not unreasonable for this type of sample, and values of $R < 20$ are unobtainable except for crystalline structures of clearly defined geometries. The estimated levels of accuracy in the refinements made by the EXCURV92 program arising from imperfect transferability of phase shifts and the fitting procedures are coordination number (50%); Debye−Waller factor, $2\sigma^2$ (50%); and radii (0.03 Å). The significance of extra shells was evaluated by using the reduced chi^2 test, $N_p = [\{(2.\Delta k.\Delta R)/\pi\} + 1]$, where N_p is the maximum number of variables and Δk and ΔR are the ranges in k- and r-space, respectively.

Results and Discussion

Powder X-ray Diffraction. X-ray diffractograms for all materials calcined at 573 K were similar, exhibiting only broad reflections due to a semicrystalline CeO_2 phase. Examination of the $Cu/Cr/CeO_2$-cop/imp (11.6:18.3:70.1) material after calcination at 873 K showed the presence of two crystalline phases: CeO_2 and Cr_2O_3. However, after calcination at 1273 K, three distinct phases were distinguishable: CeO_2 (cubic),[33] CuO (monoclinic),[34] and Cr_2O_3 (rhombohedral).[35] Diffractograms of the $Cu/Cr/CeO_2$-imp/imp (6.8:9.7:83.5) material up to a calcination temperature of 873 K showed only peaks attributable to CeO_2, but after calcination at 1273 K, the diffractogram showed very weak peaks indicative of both CuO and Cr_2O_3. No peaks due to ternary oxide phases were visible for either material, and the close correspondence of the unit cell dimensions ($a = 5.408$ Å, $V = 158.24$ Å^3) with those of the pure CeO_2[33] ($a = 5.411$ Å, $V = 158.46$ Å^3) demonstrates that no solid solution of copper or chromium in CeO_2 occurs in either material.

In contrast, the behavior of the three $Cu/Cr/CeO_2$−cop materials was quite different. The diffractogram of the 12.7:24.0:63.3 material calcined at 873 K showed the presence of two crystalline phases; the more intense phase was identified as CeO_2, while the weak, but sharper second pattern was attributed to tetragonal $CuCr_2O_4$[36] ($a = 6.054$ and $c = 7.788$ Å). No other phases, including those of the binary copper or chromium oxides, are apparent in the diffractogram. Calcination of this material at 1273 K resulted in two dramatic changes in the diffractogram. First, the peaks of the ceria phase sharpened as the average particle size increased to ca. 750 Å, and second, the $CuCr_2O_4$ phase is converted to $Cu_2Cr_2O_4$.[37] No other phases were detected.

Comparison of these data with those for the 7.4:21.5:71.1 and 13.9:11.9:74.2 materials highlights the dependence of ternary Cu/Cr oxide formation on both the Cu:Cr ratio and the calcination temperature. For the 13.9:11.9:74.2 material, the $CuCr_2O_4$ phase was once again formed at 873 K, with no evidence for a phase formed by excess copper, and again, $CuCr_2O_4$ was converted to $Cu_2Cr_2O_4$ upon heating to 1273 K together with CuO formed from excess copper. As with the other two ratios, the 7.4:21.5:71.1 material formed $CuCr_2O_4$ upon calcination at 873 K, but in this case, however, this phase appeared to be stable on calcination at 1273 K. At both temperatures, Cr_2O_3 was also evident. None of these materials showed any change in the cerium oxide pattern, with peak positions and relative intensities remaining in agreement with reference[36] data at all temperatures and compositions.

It is interesting to note that a comparison of the catalytic data for the $Cu/Cr/CeO_2$-cop materials[30] with those of the singly promoted Cu/CeO_2-cop materials show the former to exhibit superior activity for materials processed at the same temperature. Hence, we may

(29) DICVOL91, Boultif, A.; Louer, D. *J. Appl. Crystallogr.* **1991**, *24*, 987.
(30) *EXBACK*, *EXCALIB*, and *EXCURV92*; Daresbury Computer programs; Daresbury Laboratory: Cheshire, U.K., 1991.
(31) Gurman, S. J.; Binstedt, N.; Ross, I. *J. Phys. C: Solid State Phys.* **1984**, *17*, 143; **1986**, *19*, 1845.
(32) Lee, P. A.; Pendry, J. B. *Phys. Rev. B: Condens. Matter* **1975**, *11*, 2795.
(33) CeO_2 JCPDS file no. 34-394.
(34) CuO JCPDS file no. 5-661.
(35) Cr_2O_3 JCPDS file no. 38-1479.
(36) $CuCr_2O_4$ JCPDS file no. 34-424.
(37) $CuCrO_2$ JCPDS file no. 39-247.

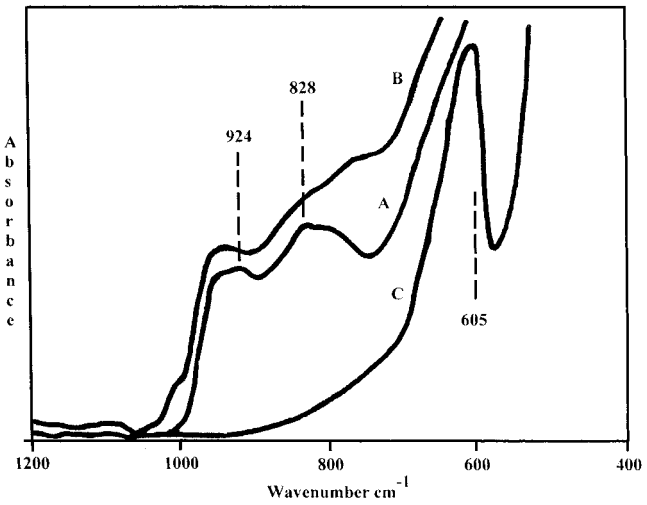

Figure 1. FTIR spectra of the Cu/Cr/CeO_2-cop (Cu:Cr:Ce 12.7:24.0:63.3) catalyst material dried at 383 K (A), after calcination at 573 K (B), and at 873 K (C).

speculate that the increased activity is due to the formation of these spinel structures in the catalyst.

Fourier Transform IR Spectroscopy. Spectra recorded for the Cu/Cr/CeO_2-imp/imp and Cu/Cr/CeO_2-cop/imp materials are very similar in appearance to those obtained for Cr(VI)/CeO_2 catalyst materials.[38] This implies that the presence of copper in the latter sample appears to have no affect on the adsorption of chromate ions onto the ceria particulate surface, and in the former, the second impregnation stage does not cause adsorbed chromate to be washed off. Spectra of samples dried at low temperature exhibited a broad envelope of peaks in the range of 700−1000 cm^{-1}, due to the Cr═O stretching vibrations due to surface adsorbed chromate-(VI) ions, which become much reduced in intensity on calcination at 573 K. All traces of surface chromate species are absent after calcination at 873 K, and spectra are dominated by an intense peak at 600 cm^{-1} associated with the lattice Cr−O stretching vibration in crystalline Cr_2O_3,[39] the intensity of which increases upon calcination at 1273 K (spectra not shown).

Spectra of the Cu/Cr/CeO_2-cop materials calcined at 383 K show two broad bands with maxima at 828 and 924 cm^{-1} in the Cr(VI)═O stretching region (Figure 1-(A)), which can be assigned to surface chromate(VI) species.[40,41] This observation demonstrates that Cr(III) in the material undergoes oxidation in part at least to Cr(VI) under relatively mild conditions (16 h calcination at 383 K). A similar conversion has been reported previously in Cr(III) impregnated titania by Scharf et al.,[42] who observed that the temperature of conversion and the chromium species formed were dependent upon the chromium loading. At low loadings (3 wt % Cr) and low temperatures (ca. 373 K), the chromium appeared to be converted to a coordinatively unsaturated surface chromyl (Cr^V) species, whereas for higher loadings (30 wt %) and higher temperatures (ca. 413 K), the conversion was into coordinatively saturated surface chromate-(VI) species. Calcination at 573 K results in a decrease in intensity of both bands (Figure 1(B)). The weak but distinct shoulder in the spectrum after calcination at 573 K at ca. 1000 cm^{-1} (Figure 1(B)) has been attributed to mononuclear Cr(V) species[43] and indicates that complete oxidation to Cr(VI) has not occurred. This observation is not too surprising considering the known surface stabilization of Cr(V).[44] By 873 K, the only feature is a broad, intense band at ca. 605 cm^{-1} (Figure 1(C)) which grows in intensity after calcination to 1273 K. Although this band is very similar to that observed for the Cu/Cr/CeO_2-imp/imp and Cu/Cr/CeO_2-cop/imp materials in which crystalline Cr_2O_3 is produced at elevated temperatures, other techniques (XRD, EXAFS) indicate that this is not formed in the Cu/Cr/CeO_2-cop (12.7:24.0:63.3) material, and in this case, we ascribe this band to crystalline $CuCr_2O_4$[45−47]and $Cu_2Cr_2O_4$. Unfortunately, the materials were too dark to obtain good quality Raman spectra.

Table 2. Refined Structural Parameters from Cu K Edge EXAFS Data for the Cu/Cr/CeO_2-Cop (12.7:24.0:63.3) Catalyst Material after Calcination at Various Temperatures in the Range of 333−1273 K[a,b]

calcination temp	atom type	coord. no.	radial dist, Å	Cu species present	lit. values, Å
333 K	O	2	1.952	$Cu(OH)_2$[c]	1.948
	O	2	1.977		1.972
	O	1	2.443		2.356
	O	1	2.924		2.915
	Cu	2	2.951		2.947
	Cu	3	3.322		3.340
873 K	O	4	1.951	$CuCr_{2O4}$[d]	1.939
	O	4	3.192		3.175
	Cr	4	3.274		3.289
	Cr	4	3.356		3.385
	O	4	3.471		3.466
	Cu	4	3.555		3.592
1273 K	O	2	1.868	Cu_{2Cr2O4}[e]	1.846
	Cu	6	2.986		2.975
	Cr	6	3.132		3.327
	O	6	3.498		3.501

[a] *R* values: 26.7 (333 K), 30.0 (873 K), and 49.4 (1273 K). [b] Average Debye−Waller factor $2\sigma^2$: 333 K, 0.008 $Å^2$ (0.004−0.035 $Å^2$); 873 K, 0.009 $Å^2$ (0.005−0.021 $Å^2$); 1273 K, 0.009 $Å^2$ (0.005−0.021 $Å^2$). [c] Reference 49. [d] Reference 50. [e] Reference 51.

X-ray Absorption Spectroscopy. *Cu K Edge EXAFS Spectra.* EXAFS data recorded for the Cu/Cr/CeO_2-cop (12.7:24.0:63.3) material dried at 383 K fitted well to $Cu(OH)_2$ (Table 2), which is the same copper species found for the Cu/CeO_2-cop material after similar thermal processing conditions.[48] Data for the Cu/Cr/CeO_2-cop/imp (11.6:18.3:70.1) material dried at 333 K also fitted reasonably well to the structural parameters of $Cu(OH)_2$ (Table 3). Attempts to fit the data to $[Cu(H_2O)_6]^{2+}$ resulted in substantially inferior fits. After thermal treatment at 573 K, attempts to fit the experimental data obtained for both samples to various phases

(38) Harrison, P. G.; Daniell, W. *Chem. Mater.* **2001**, *13*, 1708.
(39) Marshall, R.; Mitra, S. S.; Plende, J. N.; Mansur, L. C. *J. Chem. Phys.* **1965**.
(40) Mattes, R. *Z. Anorg. Allg. Chem.* **1961**, *311*, 102.
(41) Hardcastle, F. D.; Wachs, I. E. *J. Mol. Catal.* **1989**, *46*, 173.
(42) Scharf, U.; Schneider, H.; Baiker, A.; Wokaun, A. *J. Catal.* **1994**, *145*, 464.
(43) Schraml-Marth, M.; Wokaun, A.; Baiker, A. *J. Catal.* **1992**, *133*, 415.
(44) Cimino, A.; Cordischi, D.; De Rossi, S.; Valigi, M. *J. Catal.* **1991**, *127*, 761.
(45) Harrison, P. G.; Lloyd, N. C.; Daniell, W.; Ball, I. K.; Bailey, C.; Azelee, W. *Chem. Mater.* **2000**, *12*, 3113.
(46) Hafner, S. *Z. Kristallogr.* **1961**, *115*, 331.
(47) Basak, D.; Ghose, J. *Spectrochim. Acta, Part A* **1994**, *50*, 713. *43*, 2893.
(48) Harrison, P. G.; Bailey, C.; Daniell, W.; Zhao, D.; Ball, I. K.; Goldfarb, D.; Lloyd, N. C.; Azelee, W. *Chem. Mater.* **2000**, *12*, 3715.

Table 3. Refined Structural Parameters from Cu K Edge EXAFS Data for the Cu/Cr/CeO_2-cop/imp (11.6:18.3:70.1) Catalyst Material after Calcination at Various Temperatures in the Range of 333−1273 K[a,b]

calcination temp	atom type	coord. no.	radial dist, Å	Cu species present	lit. values, Å
333 K	O	2	1.944	$Cu(OH)_2$[c]	1.948
	O	2	1.969		1.972
	O	1	2.384		2.356
	O	1	2.903		2.915
	Cu	2	2.945		2.947
	Cu	3	3.330		3.340
873 K	O	2	1.959	CuO[d]	1.951
	O	2	1.965		1.961
	O	2	2.802		2.784
	Cu	4	2.995		2.901
	Cu	4	3.103		3.083
1273 K	O	2	1.959	CuO[d]	1.951
	O	2	1.965		1.961
	O	2	2.802		2.784
	Cu	4	2.995		2.901
	Cu	4	3.103		3.083
	Cu	2	3.094		3.173

[a] *R* values: 29.8 (333 K), 45.4 (873 K), and 35.5 (1273 K). [b] Average Debye−Waller factor $2\sigma^2$: 333 K, 0.008 Å^2 (0.001−0.040 Å^2); 873 K, 0.010 Å^2 (0.005−0.024 Å^2); 1273 K, 0.007 Å^2 (0.001−0.011 Å^2). [c] Reference 49. [d] Reference 52.

(e.g., $Cu(H_2O)_6^{2+}$, $Cu(OH)_2$, or CuO) proved very difficult and resulted in very poor matches. We assume that this is due to Cu occupying more than one phase (and hence, environment) at this temperature, which is most likely an amorphous form of CuO or clusters of hydrated Cu^{2+} ions. Data for the Cu/Cr/CeO_2-cop material after calcination at 873 K fits acceptably to $CuCr_2O_4$, the presence of which was indicated by XRD analysis of this sample. The discrepancies between the refined experimental and observed data can be attributed to the likely presence of CuO within the sample even though it was not detected by XRD. After calcination at 1273 K, the data for this sample fit $Cu_2Cr_2O_4$, albeit rather poorly, implying the presence of small amounts of other copper species such as $CuCr_2O_4$ and CuO. Attempted fits to either of these two phases were noticeably worse. After calcination at 873 K, the EXAFS data for the Cu/Cr/CeO_2-cop/imp material fit to CuO, although after calcination at 1273 K, the fit to CuO is significantly better.

Cr K Edge XANES Spectra. Although useful EXAFS data could not be accumulated, the nature of the Cr K absorption edge can be unequivocally diagnostic for the presence or absence of chromium in the +VI oxidation state. Chromium +VI compounds such as $Na_2CrO_4{\cdot}4H_2O$, $Na_2Cr_2O_7{\cdot}2H_2O$, and CrO_3 exhibit an intense peak ca. 4.1−4.3 eV before the main edge; however, this feature is absent in chromium(III) compounds such as $Cr_2(SO_4)_3{\cdot}12H_2O$ and $CrK(SO_4)_2{\cdot}12H_2O$.[53] For the Cr^{6+} ion, multiple scattered wave calculations have indicated that the preedge peak is due to an electronic transition from the Cr 1s orbital to an empty antibonding molecular orbital of primarily Cr 3d character.[54,55] This quadrupole, 1s → 3d, transition is "dipole-allowed" in a tetrahedral ligand field because of the extensive mixing of odd-parity Cr $3d_{z^2}$ and $4p_z$ orbitals with oxygen 2s and $2p_z$ orbitals. The intensity of the 1s → 3d transition varies with the number of d orbital vacancies, the site symmetry of the X-ray absorbing atom, and the metal−ligand bond length.[56] Hence, the observation of a preedge feature may be deemed characteristic of chromium in the +VI oxidation state coordinated tetrahedrally (by oxygen).[57,58]

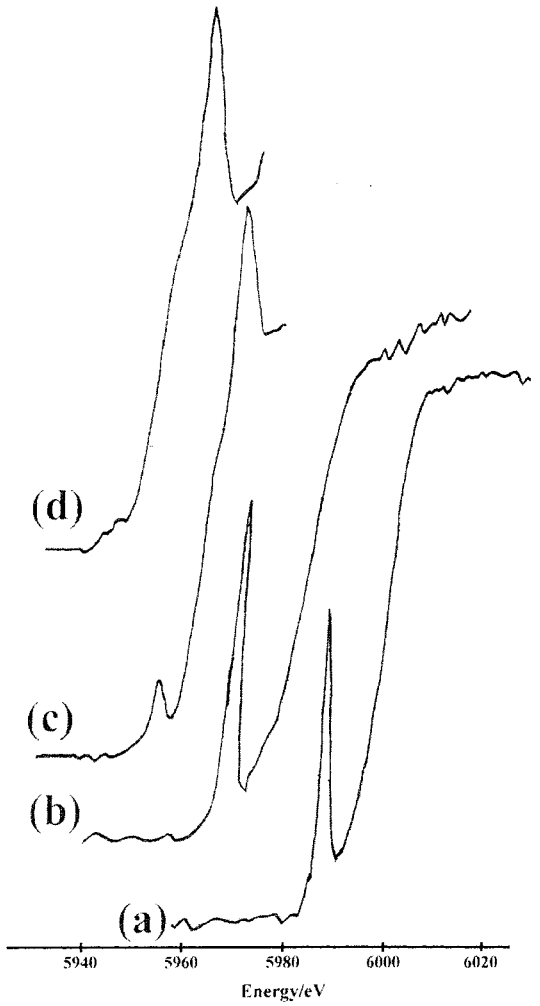

Figure 2. Cr K X-ray absorption edge of the Cu/Cr/CeO_2-cop (Cu:Cr:Ce, 12.7:24.0:63.3) material calcined at (a) 383, (b) 573, (c) 873, and (d) 1273 K. Spectra are not energy-calibrated, and spectra (b)−(d) are offset to lower energy with respect to spectrum (a) by ca. 20 eV.

XANES spectra recorded for the Cu/Cr/CeO_2-cop (12.7:24.0:63.3) material after thermal treatment at various temperatures are shown in Figure 2, with the calcination temperature increasing from the lower to the upper trace. Surprisingly, the preedge feature characteristic of Cr(VI) in a tetrahedral environment can be

(49) Oswald, H. R.; Reller, A.; Schmalle, H.; Dubler, E. *Acta Crystallogr.* **1990**, *46*, 2279.
(50) Prince, E. *Acta Crystallogr.* **1957**, *10*, 554.
(51) Hannhauser, W.; Vaughn, P. A. *J. Am. Chem. Soc.* **1955**, *77*, 896.
(52) Asbrink, S.; Lorrby, L. J. *Acta Crystallogr., Sect. B* **1970**, *26*, 8.
(53) Wainwright, J. S.; Murphy, O. J.; Antonio, M. R. *Corros. Sci.* **1992**, *33*, 281.
(54) Kutzler, F. W.; Natoli, C. R.; Misemer, D. K.; Doniach, S.; Hodgson, K. O. *J. Chem. Phys.* **1980**, *73*, 327.
(55) Penner-Hahn, J. E.; Benfatto, M.; Hedman, B.; Takahashi, T.; Doniach, S.; Groves, J. T.; Hodgson, K. O. *Inorg. Chem.* **1986**, *25*, 2255.
(56) Wong, J.; Lytle, F. W.; Messmer, R. P.; Maylotte, D. H. *Phys. Rev. B: Condens. Matter* **1984**, *30*, 5596.
(57) Hawkins, J. K.; Isaacs, H. S.; Heald, S. M.; Tranquada, J.; Thompson, G. E.; Wood, G. C. *Corros. Sci.* **1987**, *27*, 391.
(58) Miyake, M.; Nakgawa, N.; Ohyanagi, H.; Suzuki, T. *Inorg. Chem.* **1986**, *25*, 700.

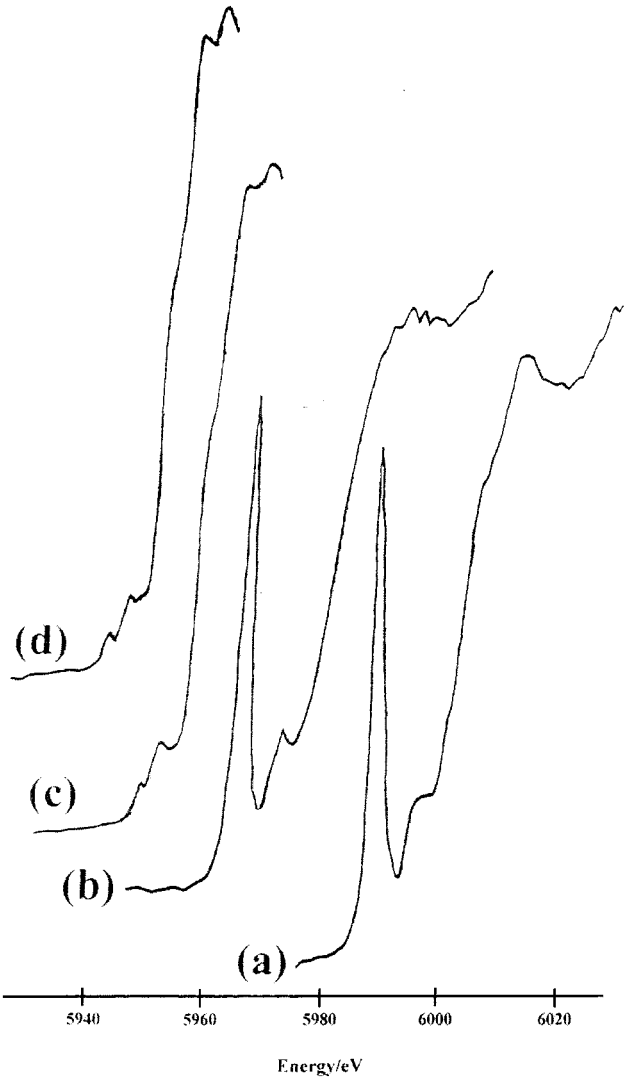

Figure 3. Cr K X-ray absorption edge of the Cu/Cr/CeO_2-cop/imp (Cu:Cr:Ce 11.6:18.3:70.1) material calcined at (a) 333 K, (b) 573 K, (c) 873 K, and (d) 1273 K. Spectra are not energy calibrated and spectra (b)−(d) are offset to lower energy with respect to spectrum (a) by ca. 20 eV.

clearly seen in the spectra for the material after treatment at 383 and 573 K, which is indicative that oxidation at least in part of the Cr(III) precursor to Cr(VI) occurs by 383 K. This is consistent with the IR data for these materials which exhibit bands at 828 and 924 cm^{-1}, which we assign to Cr(VI)═O vibrations. However, the precise nature of the Cr(VI) species is indeterminate from these data. By 873 K, there is a marked decrease in the intensity of the preedge feature, and at 1273 K, it appears to be absent.

The XANES spectra recorded for the Cu/Cr/CeO_2-cop/imp (11.6:18.3:70.1) material over the calcination temperature range of 333−1273 K are shown in Figure 3. As expected, the material dried at 333 K shows the presence of a large preedge peak, which is assigned to surface chromate(VI) species. No change is observed after calcination to 573 K, but at temperatures ≥873 K, the intensity of the preedge feature decreases significantly. Similarly, for the Cu/Cr/CeO_2-imp/imp (8.2:9.7:83.5) material, the preedge feature is prominent for the material treated at 333 and 573 K but is essentially absent by 873 K. A comparative plot of peak intensity

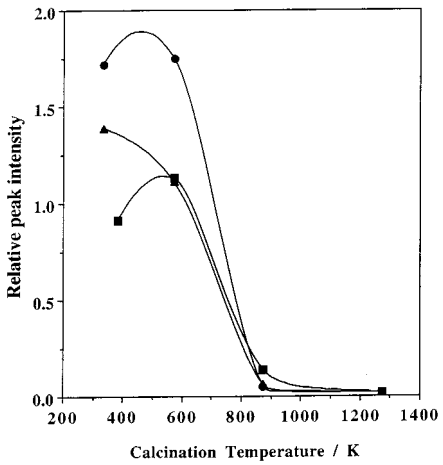

Figure 4. Plot of the variation of the peak intensity of the preedge feature with temperature for Cu/Cr/CeO_2-imp/imp (▲), Cu/Cr/CeO_2-cop/imp (●), and Cu/Cr/CeO_2-cop (■) materials.

of the preedge feature vs thermal processing temperature is shown in Figure 4. These results confirm the observations from FTIR that in the Cu/Cr/CeO_2-cop materials, thermal treatment at 333 K causes at least partial oxidation of Cr^{III} to Cr^{VI}. Oxidation of Cr(III) to Cr(VI) has been previously reported by Baker et al.,[59] during structural analysis of hydrated Cr_2O_3 gels, and by Scharf et al.[42] in chromium(III) nitrate impregnated titania materials. A similar oxidation of chromium(III) to chromium(VI) has been inferred by photoelectron spectroscopy for alumina-supported chromia catalysts.[60] Treatment at temperatures higher than 873 K causes the reversion of these Cr^{VI} species to the more thermally stable Cr^{III}, which also occurs in the Cu/Cr/CeO_2-cop/imp andCu/Cr/CeO_2-imp/imp materials.

Electron Paramagnetic Resonance. Studies by Weckhuysen et al.[61,62] on Cr(VI)/SiO_2 and Cr(VI)/Al_2O_3 catalysts have shown that three different chromium signals are observable in the EPR depending on the treatment history of the catalysts. These are referred to as the δ-, γ-, and β-signals. The δ- and β-signals are broad and occur in the g_{eff} ranges ca. 5 and 1.96−2.45, respectively. The δ-signal results from dispersed Cr^{3+} ions, whereas the β-signal is assigned to clusters of Cr^{3+}. The β-signal is strongly dependent on the size and shape of these clusters as indicated by the broad range of g values. The γ-signal is much sharper and occurs at g = 1.97. The assignment of the γ-signal is the source of much contention. Spitz[63] has attributed the signal to mixed valence trimers, $Cr^{VI}-O-Cr^{III}-O-Cr^{VI}$, with an average Cr oxidation state of +V. This assignment has been supported by other authors working on alumina-[64] and titania-supported[65] chromium oxide catalysts. However, an alternative interpretation assigns the signal to a mononuclear chromyl (Cr^{V}) complex with

(59) Baker, F. S.; Carruthers, J. D.; Stryker, L. J. *Discuss. Faraday Soc.* **1971**, *52*, 173.
(60) Park, P. W.; Ledford, J. S. *Langmuir* **1997**, *13*, 2726.
(61) Weckhuysen, B. M.; Schoonheydt, R. A.; Mabbs, F. E.; Collison, D. *J. Chem. Soc., Faraday Trans. 1* **1996**, *92*, 2431.
(62) Weckhuysen, B. M.; De Ridder, L. M.; Grobert, P. J.; Schoonheydt, R. A. *J. Phys. Chem.* **1995**, *99*, 320.
(63) Spitz, R. *J. Catal.* **1974**, *35*, 345.
(64) Ellison, A.; Singh, K. S. W. *J. Chem. Soc., Faraday Trans.* **1977**, *73*, 2807.
(65) Amorelli, A.; Evans, J. C.; Rowlands, C. C.; Egerton, T. A. *J. Chem. Soc., Faraday Trans.* **1987**, *83*, 3541.

square pyramidal coordination, which is stabilized by interaction with the support surface. This has been proposed by EPR studies of the Cr/ZrO_2[66] and $Cr/SiO_2/Al_2O_3$[61] systems.

Four different copper EPR signals have been observed for Cu/CeO_2[48] catalyst materials depending on the thermal pretreatment history. The first is a broad isotropic signal ($g_{iso} \approx 2$) observed at low calcination temperatures and is attributed to Cu^{2+} ions in the form of amorphous copper(II) aggregates present on the surface of the ceria particles (type B signal[67]). The second signal, which has an axial symmetry, is present at all temperatures and becomes more clearly resolved with increasing calcination temperature, adopting parallel and perpendicular components of the hyperfine structure. The EPR parameter values of this signal ($g_{\|} = 2.248$ and $g_{\perp} = 2.092$; $A_{\|} = 120$ and $A_{\perp} = 28$ G) are characteristic of isolated Cu^{2+} ions located in tetragonally distorted octahedral sites (type A signal[67]). The third copper signal is also isotropic ($g_{iso} = 2.098$) and is seen only with high copper concentrations and after calcination at high temperature and is attributed to CuO particles. The final signal, which appears complex, is observed after calcination at 873 K and becomes more clearly resolved at higher temperatures. This signal has been extensively studied[67,68] and attributed to copper(II) ion dimers (type K signal[67]) and exhibits fine and hyperfine structure ($g_{\|} = 2.195$, $A_{\|} = 85$ G; $g_{\perp} = 2.031$, $A_{\perp} = 12$ G) arising from the coupling between unpaired electrons of two Cu^{2+} ions ($I = {}^3/_2$). Each component of the fine structure is comprised of seven narrow lines with relative intensities of 1:2:3:4:3:2:1.

Spectra for the $Cu/Cr/CeO_2$-cop/imp (11.6:18.3:70.1) material calcined over a range of temperatures from 333 to 1273 K are illustrated in Figure 5. The upper spectrum of the material dried at 333 K comprises two well-resolved signals. The sharp, narrow line at ca. 3500 G ($g_{\perp} = 1.966$, $g_{\|} = 1.945$) grows in intensity as the sample is calcined to 573 K. The presence of a Cr γ-signal in the spectrum of the material dried at 333 K is surprising as Cr(VI) ($3d^0$) is EPR silent. Since it is unlikely that reduction of Cr(VI) to Cr(III) has taken place in this sample under these conditions (thereby creating a mixed valence species), the γ-signal is assigned to a Cr(V) species.[67] The second distinct signal is characteristic of Cu^{2+} ions with axial symmetry ($g_{\perp} = 2.028$) and has no discernible hyperfine structure. The shoulder to the low field side of this signal is due to Cu^{2+} ion clusters.

After calcination to 573 K, the two sharp signals appear superimposed upon a third, broader and less well-resolved signal ($g_{eff} \approx 2$) which is assigned as the Cr^{3+} β-signal due to clustered but amorphous Cr_2O_3.[63] The Cr γ-signal grows in intensity at this temperature, but whether this feature is due to chromyl Cr(V) species or mixed valence trimers, $Cr^{VI}-O-Cr^{III}-O-Cr^{VI}$, is equivocal. A fourth, broader ($\Delta H \approx 500$ G) signal that

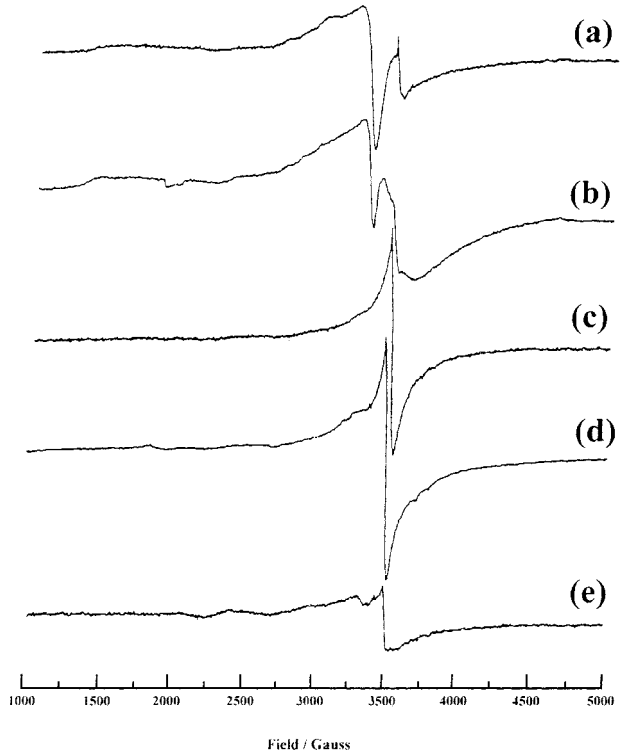

Figure 5. EPR spectra of the $Cu/Cr/CeO_2$-cop/imp (Cu:Cr:Ce, 11.6:18.3:70.1) catalyst material after calcination at (a) 333, (b) 573, (c) 873, (d) 1073, and (e) 1273 K.

is centered around 1700 G and is showing only a positive lobe is characteristic of the δ-signal[63] due to dispersed Cr^{3+} ions in highly distorted octahedral coordination ($g = 3.5-5.5$). This signal is not present in the spectra of samples calcined at higher temperatures.

The spectrum after calcination to 873 K is far less complex and appears to consist only of an intense Cr γ-signal. This line is still present after calcination to 1073 K, though it is now superimposed onto the broad isotropic Cr β-signal ($g_{iso} = 1.980$) characteristic of clusters of amorphous Cr_2O_3. Calcination to 1273 K greatly reduces the intensity of both the γ- and β-signals, as crystalline antiferromagnetic α-Cr_2O_3 is formed. The lack of a Cu^{2+} signal in the spectrum after calcination at 873 K can also be accounted for by antiferromagnetic coupling, which occurs in the CuO phase present at these calcination temperatures. None of the spectra show the presence of Ce^{3+}. These data comply with our proposal that in the $Cu/Cr/CeO_2$-cop/imp material no intimate mixing of the two transition-metal promoters occurs and that at high temperatures, two separate phases of CuO and Cr_2O_3 are formed.

The EPR spectra for the $Cu/Cr/CeO_2$-cop (12.7:24.0:63.3) material are shown in Figure 6. The spectrum of the material dried at 373 K is comprised of two signals, which are both attributable to chromium species. The sharp γ-signal ($g_{\perp} = 1.975$, $g_{\|} = 1.955$) is characteristic of isolated chromyl Cr^V species, while the broader ($\Delta H \approx 1000$ G) β-signal corresponds to isolated Cr^{3+} ions with octahedral coordination ($g_{iso} = 1.985$). The strength of these signals masks any trace of Cu^{2+} in the spectrum. However, after calcination to 573 K, the spectrum is dominated by signals associated with Cu^{2+} ionic species, although a weak Cr γ-signal can still be discerned. The main signal ($g_{\perp} = 2.032$, $g_{\|} = 2.309$)

(66) Cimino, A.; Cordischi, D.; De Rossi, S.; Valigi, M. *J. Catal.* **1991**, *127*, 761.
(67) Aboukais, A.; Bennain, A.; Aissi, C. F.; Wrobel, G.; Guelton, M.; Vedrine, M. *J. Chem. Soc., Faraday Trans.* **1992**, *88*, 615.
(68) Abi-Aad, E.; Bonnelle, J. P.; Aboukais, A. *J. Chem. Soc., Faraday Trans.* **1995**, *91*, 99.
(69) Chien, C. C.; Cheung, W. F.; Hueng, T. J. *Appl. Catal., A* **1995**, *131*, 73.

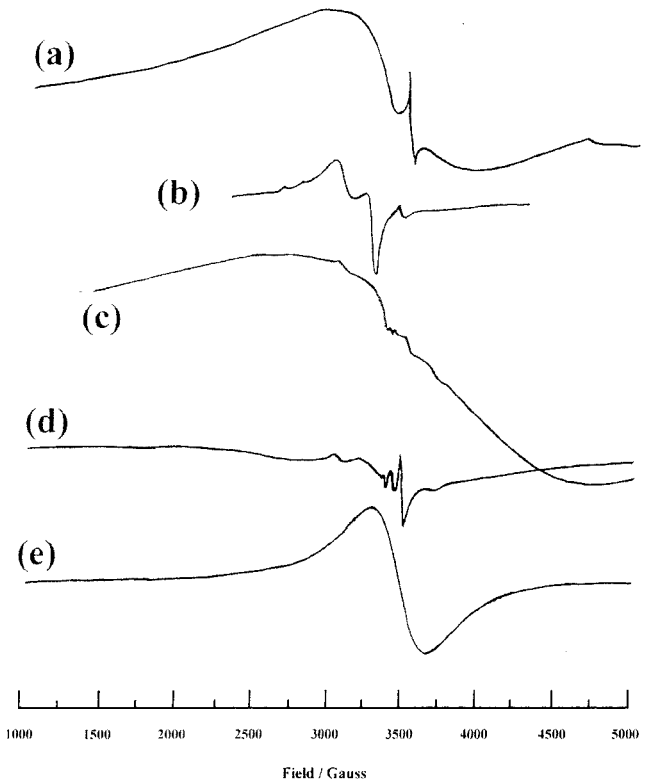

Figure 6. EPR spectra of the $Cu/Cr/CeO_2$-cop (Cu:Cr:Ce, 12.7:24.0:63.3) catalyst material after calcination at (a) 383, (b) 573, (c) 873, (d) 1073, and (e) 1273 K.

indicative of Cu^{2+} ions with axial symmetry[68] is superimposed upon a broader, isotropic signal ($\Delta H \approx 200$ G) characteristic of clustered Cu^{2+} ions. The low field shoulders are part of the poorly resolved hyperfine splitting in the parallel section of the axial signal ($A_{\parallel} =$ 90 G). The Cr γ-signal is significantly reduced in intensity and remains so until after calcination to 1073 K, when its intensity increases.

Resolution in the spectrum of the material calcined at 873 K is generally poor, as all signals are partially masked by the very broad ($\Delta H \approx 3200$ G) β-signal associated with Cr^{3+} ions ($g_{\text{eff}} \approx 2$). It appears that calcination at 873 K brings about dramatic changes within this sample. The Cr δ-signal is absent, and two new signals at ≈3000 and 3700 G characteristic of Cu^{2+} dimers (type K signal) are now apparent which become more prominent at 1073 K. Calcination to 1273 K produces a single, intense isotropic signal ($g_{\text{iso}} = 1.980$, $H = 700$ G) associated with the Cr β-signal due to clustered octahedral Cr^{3+} ions (cf. the EPR spectrum of the $Cu/Cr/CeO_2$-cop/imp material calcined at 1273 K). Under these thermal processing conditions, both XRD and EXAFS indicate the presence of $Cu_2Cr_2O_4$ in which the copper is in oxidation state +I and therefore is EPR silent. Hence, the observation of a Cr β-signal under these conditions is quite consistent with these data.

Summary

Three methods may be employed to prepare copper and chromium doubly promoted ceria catalysts:

(i) by coprecipitation from aqueous solutions containing cerium(IV), copper(II), and chromium(III) ions.

(ii) by dual impregnation of CeO_2 by using an aqueous CrO_3 solution, followed by drying and impregnation of the yellow powder obtained by using an aqueous solution of copper(II) nitrate, and

(iii) by impregnation of $Cu(II)/CeO_2$ prepared by coprecipitation by using an aqueous CrO_3 solution.

All three types of material are quite different in appearance, and in all cases, the loading of copper is significantly lower than the "target" level whereas that of chromium is reasonably close to the expected value (Table 1).

The constitutional nature of the $Cu/Cr/CeO_2$-cop catalyst material after thermal processing in the temperature range of 383−1273 K is summarized in Table 4. At 383 K, in the $Cu/Cr/CeO_2$-cop (12.8:24.0:63.3) catalyst material the copper is present as (polymeric) $Cu(OH)_2$, but the chromium is present as isolated Cr^{3+} ions, isolated chromyl Cr^{V} species, and a Cr^{VI} species, which is most likely a surface chromate species. This would indicate that a degree of oxidation of the Cr^{III} has taken place during the drying stage at 333 K. Thermal processing at 573 K reduces the amount of the chromyl and chromate species, but both isolated and clustered Cu^{2+} ions are formed indicating the depolymerization of $Cu(OH)_2$. We conclude that at processing temperatures up to 573 K, there is no interaction between the Cu and Cr promoters and that at 573 K, the material is comprised of crystallites of ceria which are ca. <10 nm in size that are supporting amorphous copper(II) and chromium(III), chromium(V), and chromium(VI) oxide species. The $CuCrO_4$ phase containing Cr^{VI} has been shown to be formed in both the $Cu/Cr/SnO_2$[42] and $Cu/Cr/\gamma-Al_2O_3$[67] systems at temperatures around 573 K. However, it is equivocal whether this phase is formed in this material, although the observation of chromium(VI) and chromate(VI) in the XANES and the FTIR spectra , respectively, lends some support.

By 873 K, however, significant changes, both physical and chemical, have occurred in the material, which now is comprised of crystallites of CeO_2 and the spinel $CuCr_2O_4$ that is <10 nm in dimension. This is generally consistent with the Cu:Cr atom ratio in this material (1:1.88). No chromium(VI) is present, but the EPR spectrum indicates the presence of Cu^{2+} dimers presumably arising from the small amounts of copper stabilized on the surface but not incorporated within the spinel. At 1273 K, the material is comprised of crystalline CeO_2 and $Cu_2Cr_2O_4$ in a range of sizes (10−300 nm), and no other species can be distinguished. Both the $Cu/Cr/CeO_2$-cop (7.4:21.5:71.1 and 13.9:11.9:74.2) catalyst materials also exhibit the formation of the spinel $CuCr_2O_4$ at 873 K. However, in addition, the former, which has a Cu:Cr atom ratio of ca. 1:3, i.e., excess chromium, forms crystalline Cr_2O_3 at temperatures of 873−1273 K. No phase-separated CuO is apparent at 873 K in the latter material which has a Cu:Cr atom ratio of ca. 1:1, but crystalline $Cu_2Cr_2O_4$ and CuO are formed after processing at 1273 K.

The constitutional nature of the $Cu/Cr/CeO_2$-cop/imp and $Cu/Cr/CeO_2$-imp/imp catalyst materials after thermal processing in the temperature range of 333−1273 K is summarized in Table 5. Both materials have a similar Cu:Cr atom ratio (ca. 1:1.5), although the loading of the former is approximately twice that of the latter. In both, at 333 K, the chromium is present as $\{Cr_2O_7^{2-}\}$ ions adsorbed onto the surface of ceria particles. The

Table 4. Summary of Constitutional Nature of the Cu/Cr/CeO_2-cop Materials

calcination temp	7.4:21.5:71.1	Cu:Cr:Ce atom ratio, 12.7:24.0:63.3	13.9:11.9:74.2
383 K		Crystallite size 3 nm (TEM) Cu present as $Cu(OH)_2$ (EXAFS), Cr(VI) present (XANES/IR). EPR shows Cr γ-signal + broad β-signal (Cu signals masked)	
573 K	CeO_2 (only crystalline phase present)	CeO_2 only crystalline phase present. Crystallite size 3 nm (TEM) Cr(VI) present (XANES). EPR spectrum dominated by Cu^{2+} ions superimposed on Cu^{2+} clusters. Cr γ-signal reduced in intensity	CeO_2 only crystalline phase present
873 K	XRD shows crystalline $CuCr_2O_4$ and Cr_2O_3	Material comprises crystalline CeO_2 and $CuCr_2O_4$ particles and no others (XRD). Crystallite size 3−10 nm (TEM) EXAFS shows $CuCr_2O_4$. XANES shows no Cr(VI). EPR shows broad Cr β-signal together with Cu^{2+} clusters and Cu^{2+} ion dimers.	Shows crystalline $CuCr_2O_4$ (no evidence for CuO from XRD)
1273 K	XRD shows crystalline $CuCr_2O_4$ and Cr_2O_3	Material comprises crystalline CeO_2 and $Cu_2Cr_2O_4$ particles and no others (XRD). Crystallite size 10−300 nm (TEM) EXAFS shows $Cu_2Cr_2O_4$. XANES shows no Cr(VI). EPR shows Cr β-signal but no Cu signal.	Shows crystalline $Cu_2Cr_2O_4$ and CuO (XRD)

Table 5. Summary of the Constitutional Nature of the Cu/Cr/CeO_2-Cop/Imp (11.6:18.3:70.1) and Cu/Cr/CeO_2-Imp/Imp (6.8:9.7:83.5) Materials

calcination temp	Cu/Cr/CeO_2-cop/imp	Cu/Cr/CeO_2-imp/imp
333 K	Chromium present as $\{Cr_2O_7^{2-}\}$ adsorbed on ceria particles(IR). Cu present as $Cu(OH)_2$ (EXAFS). Cr(VI) present (XANES). EPR shows Cr γ-signal together with isolated Cu^{2+} ions and Cu^{2+} clusters.	Chromium present as $\{Cr_2O_7^{2-}\}$ adsorbed on ceria particles(IR). Cr(VI) present (XANES)
573 K	CeO_2 only crystalline phase present (XRD). Adsorbed $\{Cr_2O_7^{2-}\}$ largely decomposed (IR). Cr(VI) present (XANES). Cr γ-signal grows in intensity, also Cr β- and δ-signals.	CeO_2 only crystalline phase present (XRD). Adsorbed $\{Cr_2O_7^{2-}\}$ largely decomposed (IR). Cr(VI) present (XANES)
873 K	Crystalline CeO_2 and Cr_2O_3 present (XRD). EXAFS shows CuO. XANES shows no Cr(VI). No $\{Cr_2O_7^{2-}\}$ present (IR). EPR shows only an intense Cr γ-signal.	CeO_2 and Cr_2O_3 present (XRD). No $\{Cr_2O_7^{2-}\}$ present. (IR) XANES shows no Cr(VI).
1073 K	EPR shows Cr γ-signal and broad β-signal.	
1273 K	Crystalline CeO_2, Cr_2O_3 and CuO present (XRD). EXAFS shows CuO. XANES shows no Cr(VI). Intensity of both Cr γ- and β-signals reduced.	CeO_2 together with weak Cr_2O_3 and CuO (XRD). XANES shows no Cr(VI)

copper is present as $Cu(OH)_2$ in the Cu/Cr/CeO_2-cop/imp material (cf. the Cu/Cr/CeO_2-cop material), and it is probably present as adsorbed hexa-aquo Cu^{2+} ions in the Cu/Cr/CeO_2-imp/imp material. At 573 K, the adsorbed $\{Cr_2O_7^{2-}\}$ ions are largely decomposed in both materials, although chromium(VI) is still present in substantial quantities. It is extremely doubtful that $CuCrO_4$ is formed in these materials since only binary oxides are formed after processing at higher temperatures. The Cu/Cr/CeO_2-cop/imp material also contains Cr as chromyl(V) and isolated and clustered chromium(III) ions. Like the Cu/Cr/CeO_2-cop materials, no chromium(VI) is present after thermal processing at 873 K, but in stark contrast, no ternary oxide phases are formed and instead phase-separated Cr_2O_3 and CuO are formed at temperatures of 873−1273 K.

Conclusions

1. The nature of the promoters varies substantially with the thermal processing temperature, the preparative route, and the Cu/Cr content. At low processing temperatures, copper is present as (polymeric) $Cu(OH)_2$ in both the Cu/Cr/CeO_2-cop and Cu/Cr/CeO_2-cop/imp materials. Chromium is present as adsorbed $\{Cr_2O_7^{2-}\}$ ions in the Cu/Cr/CeO_2-imp/imp and Cu/Cr/CeO_2-cop/imp materials, but a variety of chromium species in oxidation states +III, +V and +VI are present in the Cu/Cr/CeO_2-cop material.

2. After thermal processing at 573 K, the Cu/Cr/CeO_2-cop material is comprised of crystallites of ceria incorporating amorphous copper(II) and chromium(III), chromium(V), and chromium(VI) oxide species. At 573 K, the adsorbed $\{Cr_2O_7^{2-}\}$ ions are largely decomposed in both Cu/Cr/CeO_2-cop/imp and Cu/Cr/CeO_2-imp/imp, although chromium(VI) is still present in substantial quantities.

3. By 873 K, significant physical and chemical changes occur in the Cu/Cr/CeO_2-cop material which is comprised of crystallites of CeO_2 and the spinel $CuCr_2O_4$ which is converted at 1273 K to $Cu_2Cr_2O_4$, except when the Cu:Cr atom ratio is ca. 1:3 when separation of the crystalline Cr_2O_3 phase occurs.

4. No ternary oxide phases are formed in either the Cu/Cr/CeO_2-cop/imp or Cu/Cr/CeO_2-imp/imp materials on thermal processing at high temperatures, and only phase-separated Cr_2O_3 and CuO are formed at temperatures of 873−1273 K.

Acknowledgment. We thank the Commission of the European Community (Contract No. AVI* CT92-0012) and the EPSRC (Research Grant No. GR/J76026 and provision of facilities at DRAL) for support. We thank Dr. N.C. Lloyd and Dr. C. Bailey for assistance with the EXAFS measurements.

CM0110122